Acta Crystallographica Section B
Structural Science
ISSN 0108-7681

A conformational polymorphic transition in the high-temperature ε-form of chlorpropamide on cooling: a new ε'-form

Tatiana N. Drebushchak,[a,b]* Yury A. Chesalov[a,c] and Elena V. Boldyreva[a,b]

[a]Novosibirsk State University, REC-008, Pirogova 2, Novosibirsk 90, Russia, [b]Institute of Solid State Chemistry and Mechanochemistry SB RAS, Kutateladdze 18, Novosibirsk 128, Russia, and [c]Boreskov Institute of Catalysis SB RAS, Lavrent'eva 5, Novosibirsk 90, Russia

Correspondence e-mail: tanya@xray.nsu.ru

Received 19 June 2009
Accepted 18 August 2009

Structural changes in the high-temperature ε-polymorph of chlorpropamide, 4-chloro-*N*-(propylaminocarbonyl)benzenesulfonamide, $C_{10}H_{13}ClN_2O_3S$, on cooling down to 100 K and on reverse heating were followed by single-crystal X-ray diffraction. At temperatures below 200 K the phase transition into a new polymorph (termed the ε'-form) has been observed for the first time. The polymorphic transition preserves the space group $Pna2_1$, is reversible and is accompanied by discontinuous changes in the cell volume and parameters, resulting from changes in molecular conformation. As shown by IR spectroscopy and X-ray powder diffraction, the phase transition in a powder sample is inhomogeneous throughout the bulk, and the two phases co-exist in a wide temperature range. The cell parameters and the molecular conformation in the new polymorph are close to those in the previously known α-polymorph, but the packing of the z-shaped molecular ribbons linked by hydrogen bonds inherits that of the ε-form and is different from the packing in the α-polymorph. A structural study of the α-polymorph in the same temperature range has revealed no phase transitions.

1. Introduction

Polymorphism of drugs is a hot topic (Brittain, 1999; Bernstein, 2002; Hilfiker, 2006). From a practical point of view, the control of the polymorphism of drugs is important to obtain new pharmaceutical forms with improved properties, to prevent undesirable phase transformations on processing and on storage, and for patenting. From a fundamental point of view, the control of polymorphism of drugs is important for understanding the structure–properties relations, for crystal engineering, for polymorph prediction based on theoretical modeling of intermolecular potentials, and for studies of the thermodynamics and kinetics of the crystallization of molecular solids and of the solid-state transformations.

Chlorpropamide, 4-chloro-*N*-(propylaminocarbonyl)benzenesulfonamide (I), is an antidiabetic drug which is widely used as a model system for studying the polymorphism of molecular crystals with flexible molecules, the functional groups of which are able to form intermolecular hydrogen bonds. Several 'forms' of this compound were described in the literature long before the crystal structures of these forms were solved (Simmons *et al.*, 1973; Burger, 1975; Al-Saieq & Riley, 1982; Ueda *et al.*, 1984; De Villiers & Wurster, 1999). At the present time, the crystal structures have been solved and refined for five polymorphs of chlorpropamide: the commercially available form (Koo *et al.*, 1980) termed the α-form in Drebushchak, Chukanov & Boldyreva (2006), the β-form (Drebushchak, Chukanov & Boldyreva, 2006), the γ-form (Drebushchak *et al.*, 2007), and the δ- and ε-forms

Table 1
Selected characteristics of the crystal structures of the chlorpropamide polymorphs.

References are given in the text.

Polymorph	α	β	γ	δ	ε	ε'†
Crystal system	Orthorhombic	Orthorhombic	Monoclinic	Orthorhombic	Orthorhombic	Orthorhombic
Space group, Z	$P2_12_12_1$, 4	*Pbcn*, 8	$P2_1$, 2	*Pbca*, 8	$Pna2_1$, 4	$Pna2_1$, 4
D_{calc} (Mg m^{-3})	1.450 1.482‡	1.389	1.416	1.455	1.375	1.467‡
Orientation of the alkyl tail	I	II	II	I	II	I
Conformation of the propyl tail	*trans*	*trans*	*trans*	*gauche*	*trans*	*trans*
Hydrogen-bonded ribbon type	z	π	z	z	z	z

† To facilitate a comparison, the data for the ε'-form obtained in the present study are included in the same table. See §3. ‡ At 200 K (present study).

(Drebushchak, Chukanov & Boldyreva, 2008). All these polymorphs can exist at ambient conditions.

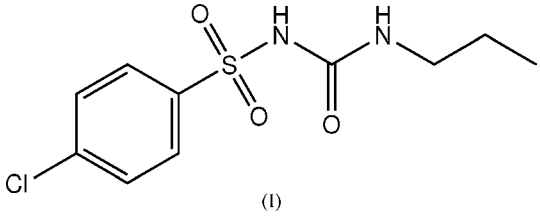

(I)

A common feature of the crystal structures of all the polymorphs is the presence of the infinite hydrogen-bonded ribbons (Fig. 1). The polymorphs differ by molecular conformations, by the mutual juxtaposition of molecules within a ribbon, and by the packing of the ribbons in the crystal structure (Table 1). Depending on the orientation of the alkyl tail and the aromatic ring with respect to the N1/C7/N2 plane, the molecular conformation has been classified as (I) (on the different sides of the plane), or as (II) (on the same side of the plane). In the four polymorphs the propyl tail itself has the *trans* conformation, and in the δ-polymorph the *gauche* conformation. In all the polymorphs one N—H group forms a relatively short hydrogen bond (1) with the C═O group of a neighboring molecule, another N—H group – a bifurcated hydrogen bond [(2) and (3)] with the same C═O group – and with an O atom of the SO_2 group of the same neighboring molecule (Fig. 1). The aromatic rings of the neighboring molecules in a hydrogen-bonded ribbon can be on different sides of the plane of the hydrogen bonds, forming a z-shaped motif, or on the same side (a π-shaped motif). Despite the same z-shaped motif, the ribbons in the α-, γ-, δ- and ε-polymorphs pack differently, and this results in different space-group symmetry.

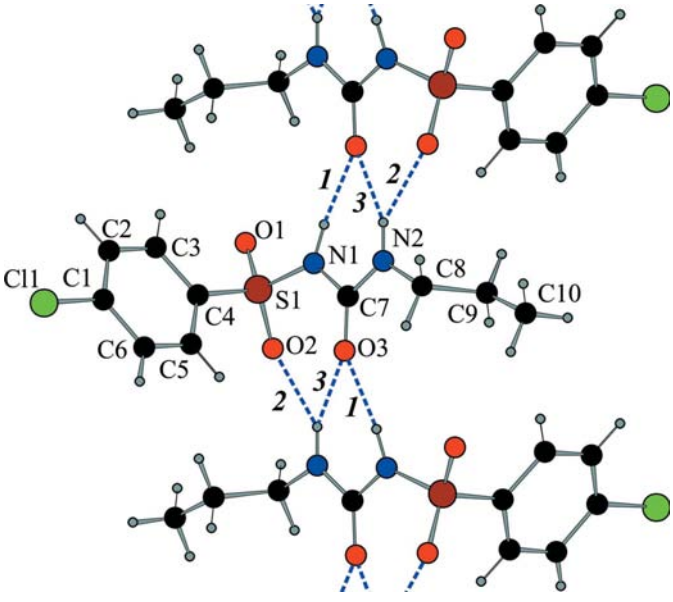

Figure 1
A fragment of a hydrogen-bonded ribbon in the crystal structures of the chlorpropamide polymorphs and the atom-numbering scheme. Hydrogen bonds are shown by dotted lines.

All five polymorphs could be obtained by crystallization from solution, often concomitantly. The ε-polymorph could be obtained from hot solutions in different solvents (Drebushchak, Chukanov & Boldyreva, 2008), and the same polymorph forms from the α-, β-, γ- and δ-polymorphs in the solid state on heating up to 398 K, just a few degrees below the melting point of the ε-polymorph at 401 K (Vemavarapu *et al.*, 2002; Drebushchak, Drebushchak, Chukanov & Boldyreva, 2008). The solid-state transitions between the polymorphs on heating from the ambient temperature up to the melting point and on reverse cooling back to ambient conditions have been studied in detail by differential scanning calorimetry (DSC), IR spectroscopy and X-ray diffraction (Drebushchak, Drebushchak, Chukanov & Boldyreva, 2008; Chesalov *et al.*, 2008). At the same time, to the best of our knowledge, structural changes in the chlorpropamide polymorphs on cooling below ambient temperature have never been studied, although at low temperatures the possibility of changing molecular conformations while preserving the packing motif and thus giving rise to new conformational polymorphs can be expected to be even higher than on heating.

The aim of the present study was to follow the structural changes in the high-temperature ε-polymorph on cooling down to 100 K. This polymorph has been selected to start a series of structural investigations into the chlorpropamide polymorphs at low temperatures, since it is preserved for a significant period of time as a metastable phase on cooling

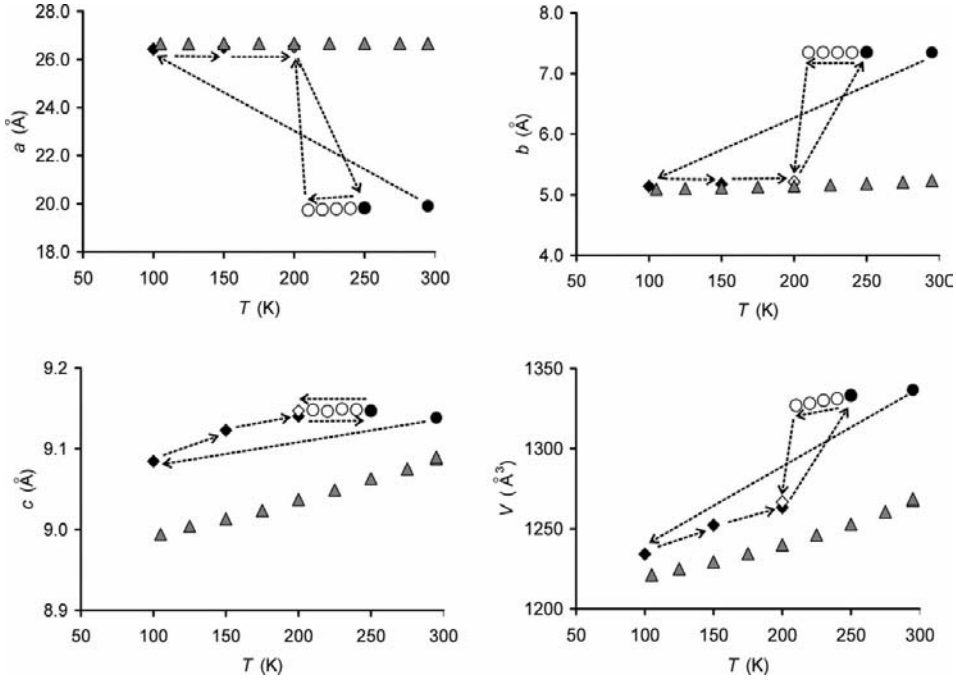

Figure 2
Cell parameters and volume of the chlorpropamide crystal *versus* temperature; circles – the ε-form, rhombs – the ε'-form; filled black symbols – the first cooling–heating cycle, open symbols – the second cooling; triangles – data for the α-polymorph. Arrows indicate the sequence of temperature changes.

from $\sim$ 398 K down to ambient temperature (Drebushchak, Drebushchak, Chukanov & Boldyreva, 2008; Chesalov *et al.*, 2008); it was also of interest to see what happens when the polymorph was cooled down further. As a result of the study, a new polymorph (ε'-form) was obtained. Since the cell parameters, the molecular conformation and the z-type of hydrogen-bonded ribbons in this new polymorph turned out to be similar to those in the stable α-polymorph (despite the difference in the space-group symmetry), the structure of the α-form was also studied on cooling and the details compared with those for the ε- and ε'-forms.

2. Experimental

2.1. Samples

Single crystals of the ε-polymorph have been obtained by the recrystallization of a commercial powder sample (α-form) from hot (373 K) chloroform solution, as was described in Drebushchak, Chukanov & Boldyreva (2008). The crystal studied in this work was the same crystal as was used for the structure determination of the ε-form at ambient temperature (Drebushchak, Chukanov & Boldyreva, 2008). The polycrystalline sample of the ε-polymorph for X-ray powder diffraction and IR spectroscopy studies was prepared by heating the commercial powder sample (α-form, the particle size is in the range 4–84 µm) in the solid state (Drebushchak, Drebushchak, Chukanov & Boldyreva, 2008). The single crystals of the α-form have been crystallized from the solution of chlorpropamide in heptane/ethyl-acetate on slow cooling from 338 K down to ambient temperature.

2.2. X-ray diffraction

A variable-temperature single-crystal X-ray diffraction study of the ε-polymorph of chlorpropamide was carried out using an Oxford Diffraction KM-4 diffractometer with a two-dimensional detector Ruby CCD (graphite monochromator, Mo $K\alpha$ radiation, λ = 0.71073 Å) with a low-temperature Oxford Instruments Cryojet device. A single crystal of the ε-polymorph was cooled from ambient temperature down to 100 K in less than an hour, after which the data were collected. Structure solution and refinement have shown that a new polymorph (defined as the ε'-form) was formed. After that, the crystal was heated up to 250 K in 50 K steps, and then cooled back down to 200 K in 10 K steps, with cell parameters being determined at each temperature point (Fig. 2). The crystal structures were solved and refined at 200 (ε'-polymorph) and 250 K (ε-polymorph). *CrysAlis* software (Oxford Diffraction, 2008*a*,*b*) was used for cell refinement, data collection and processing. After the phase transition, the crystallites within the crystal became somewhat misorientated, resulting in the data quality decreasing steadily with every cooling–heating cycle that followed.

A single-crystal diffraction study of the α-polymorph of chlorpropamide was carried out using a four-circle Stoe STADI4 diffractometer (scintillation counter, graphite monochromator, Mo $K\alpha$ radiation, λ = 0.71073 Å) with a low-temperature Oxford Cryosystems device (600 Series). A single crystal was cooled from ambient temperature down to 105 K, the cell parameters were measured every 25 K (Fig. 2), data sets for structure solution and refinement have been collected at 295, 200 and 105 K. *STADI*4 and *X-RED* (Stoe & Cie, 1997*a*,*b*) were used for cell refinement, data collection and processing.

Selected crystallographic parameters, data collection and refinement details are summarized in Table 2.[1] The directions of the crystallographic axes in the structure of the α-polymorph were chosen to facilitate a comparison of the crystal structures of the α-, ε- and ε'-polymorphs. All the structures were solved by direct methods using *SHELXS* (Sheldrick, 2008) and refined on F^2 with all data using *SHELXL* (Shel-

[1] Supplementary data for this paper are available from the IUCr electronic archives (Reference: GP5033). Services for accessing these data are described at the back of the journal.

Table 2
Experimental details.

For all structures: $C_{10}H_{13}ClN_2O_3S$, $M_r = 276.73$, $Z = 4$. Experiments were carried out with Mo $K\alpha$ radiation. Refinement was on 155 parameters. H-atom parameters were constrained.

	ε'-form of (I), 100 K	ε-form of (I), 250 K, after a reverse phase transition	ε'-form of (I), 200 K, second cooling
Crystal data			
Cell setting, space group	Orthorhombic, $Pna2_1$	Orthorhombic, $Pna2_1$	Orthorhombic, $Pna2_1$
Temperature (K)	100	250	200
a, b, c (Å)	26.4353 (19), 5.1398 (4), 9.0845 (6)	19.805 (2), 7.3500 (7), 9.1295 (9)	26.455 (4), 5.1924 (9), 9.1219 (11)
V (Å^3)	1234.33 (15)	1329.0 (2)	1253.0 (3)
μ (mm^{-1})	0.48	0.44	0.47
Crystal size (mm)	0.40 × 0.15 × 0.03	0.40 × 0.15 × 0.03	0.40 × 0.15 × 0.03
Data collection			
Diffractometer	Oxford Diffraction KM4 CCD	Oxford Diffraction KM4 CCD	Oxford Diffraction KM4 CCD
Data collection method	ω scans	ω scans	ω scans
Absorption correction	Multi-scan *CrysAlis RED* (Oxford Diffraction, 2008*b*)	Multi-scan *CrysAlis RED* (Oxford Diffraction, 2008*b*)	Multi-scan *CrysAlis RED* (Oxford Diffraction, 2008*b*)
T_{min}, T_{max}	0.800, 0.986	0.765, 0.987	0.808, 0.986
No. of measured, independent and observed [$I > 2\sigma(I)$] reflections	4372, 1995, 1399	5838, 1247, 714	4998, 1181, 630
R_{int}	0.057	0.075	0.110
θ_{max} (°)	25.0	25.0	25.0
Refinement			
$R[F^2 > 2\sigma(F^2)]$, $wR(F^2)$, S	0.047, 0.088, 0.97	0.044, 0.098, 0.85	0.054, 0.127, 0.90
No. of reflections	1995	1247	1181
No. of restraints	1	1	1
$\Delta\rho_{max}$, $\Delta\rho_{min}$ (e Å^{-3})	0.43, −0.31	0.30, −0.26	0.44, −0.25
Absolute structure	Flack (1983)	Merged equivalents	Merged equivalents
Flack parameter	0.17 (11)	–	–

	α-form of (I), 295 K	α-form of (I), 200 K	α-form of (I), 105 K
Crystal data			
Cell setting, space group	Orthorhombic, $P2_12_12_1$	Orthorhombic, $P2_12_12_1$	Orthorhombic, $P2_12_12_1$
Temperature (K)	295	200	105
a, b, c (Å)	26.673 (6), 5.2296 (19), 9.088 (2)	26.675 (5), 5.1438 (14), 9.0370 (16)	26.657 (6), 5.0938 (16), 8.9941 (18)
V (Å^3)	1267.6 (6)	1240.0 (5)	1221.3 (5)
μ (mm^{-1})	0.46	0.47	0.48
Crystal size (mm)	0.32 × 0.23 × 0.15	0.32 × 0.23 × 0.15	0.32 × 0.23 × 0.15
Data collection			
Diffractometer	Stoe STADI4 four-circle diffractometer D094	Stoe STADI4 four-circle diffractometer D094	Stoe STADI4 four-circle diffractometer D094
Data collection method	ω–2θ scans	ω–2θ scans	ω–2θ scans
Absorption correction	ψ scan	ψ scan	ψ scan
T_{min}, T_{max}	0.888, 0.937	0.886, 0.937	0.886, 0.937
No. of measured, independent and observed [$I > 2\sigma(I)$] reflections	2974, 2485, 1828	2631, 2181, 1794	2875, 2397, 2041
R_{int}	0.024	0.029	0.080
θ_{max} (°)	26.0	25.0	26.0
Refinement			
$R[F^2 > 2\sigma(F^2)]$, $wR(F^2)$, S	0.051, 0.116, 1.13	0.039, 0.092, 1.10	0.041, 0.136, 1.06
No. of reflections	2485	2181	2397
No. of restraints	0	0	0
$\Delta\rho_{max}$, $\Delta\rho_{min}$ (e Å^{-3})	0.22, −0.25	0.28, −0.27	0.30, −0.45
Absolute structure	Flack (1983)	Flack (1983)	Flack (1983)
Flack parameter	−0.01 (14)	0.00 (12)	−0.09 (15)

drick, 2008). H atoms were located in difference maps or were positioned geometrically and refined with a riding model. The absolute structure was not determined, but for the α-polymorph and for the starting ε-polymorph the values of the Flack parameter (Flack, 1983) were very reasonable [−0.01 (14) and 0.07 (8) at ambient temperature]. For the structures of the ε- and ε'-forms after the temperature cycling, the Flack parameter values were noticeably worse owing to the crystallite disorder. In the final refinement of the structural model for the ε-form at 250 K and the ε'-form at 200 K the Friedel reflections were merged.

X-ray powder diffraction data at variable temperatures have been collected using a Stoe Stadi-MP diffractometer (linear PSD detector, Ge monochromator, Cu $K\alpha_1$ radiation,

Table 3
Selected torsion angles (°) in the ε-, ε'-, α-polymorphs of chlorpropamide at several temperatures.

Since the conformational enantiomers of the molecule are not separable and sometimes occur in the same crystal all the values for a polymorph (*i.e.* for columns of ε- and ε'-forms in the table) may be multiplied by −1.

	ε†, 295 K	ε, 250 K	ε', 200 K	ε', 100 K	α, 295 K	α, 200 K	α, 105 K
O2—S1—C4—C3	162.8 (3)	162.0 (5)	−149.3 (7)	−147.2 (4)	146.0 (4)	146.0 (3)	145.6 (3)
O1—S1—C4—C3	−65.8 (3)	−66.4 (6)	−18.7 (8)	−15.7 (4)	15.0 (4)	14.9 (3)	14.2 (4)
N1—S1—C4—C3	44.6 (3)	43.6 (6)	92.9 (7)	95.8 (4)	−96.6 (4)	−96.7 (3)	−97.3 (4)
O2—S1—C4—C5	−17.4 (3)	−16.2 (6)	36.0 (8)	33.5 (4)	−35.1 (4)	−34.3 (3)	−34.3 (4)
O1—S1—C4—C5	114.0 (3)	115.3 (5)	166.6 (6)	165.0 (4)	−166.2 (4)	−165.4 (3)	−165.7 (3)
N1—S1—C4—C5	−135.7 (3)	−134.6 (5)	−81.9 (7)	−83.5 (4)	82.2 (4)	83.0 (3)	82.8 (4)
O3—C7—N1—S1	25.3 (4)	25.7 (7)	11 (1)	12.3 (6)	−8.8 (6)	−9.8 (5)	−9.4 (6)
N2—C7—N1—S1	−155.7 (2)	−154.8 (4)	−168.5 (5)	−168.8 (3)	170.2 (3)	170.1 (3)	170.2 (3)
O2—S1—N1—C7	−62.6 (3)	−63.0 (5)	−40.4 (8)	−40.2 (4)	39.5 (4)	40.1 (3)	39.7 (4)
O1—S1—N1—C7	168.1 (2)	168.0 (4)	−170.9 (6)	−171.1 (3)	169.8 (3)	170.0 (3)	169.8 (4)
C4—S1—N1—C7	54.1 (3)	54.0 (5)	75.4 (8)	74.9 (4)	−76.2 (4)	−75.7 (3)	−75.9 (4)
O3—C7—N2—C8	−3.0 (5)	−2.5 (9)	−0.5 (12)	−2.2 (7)	3.7 (7)	2.8 (6)	2.2 (7)
N1—C7—N2—C8	178.0 (3)	178.0 (5)	179.1 (6)	179.0 (3)	−175.3 (4)	−177.1 (3)	−177.4 (4)
C9—C8—N2—C7	−88.9 (5)	−89.5 (8)	102 (1)	100.4 (5)	−104.1 (5)	−102.0 (4)	−101.1 (5)
N2—C8—C9—C10	−179.4 (4)	179.8 (7)	175.0 (8)	174.8 (4)	−176.1 (4)	−175.1 (3)	−175.3 (4)

† These values are given for a comparison from Drebushchak, Chukanov & Boldyreva (2008).

λ = 1.5406 Å). The data were collected in the transmission mode from a sample in the capillary (0.5 mm diameter), which was cooled by a dry N_2 stream from an Oxford Cryosystems, 700 Series device. Cooling–heating was carried out in a 'ramp-hold' manner, with 50 or 25 K steps with the temperature changed at a rate of 120 K h^{-1} between the steps (the measurement time at every step equal to 30 min). The temperature was not measured at the sample directly. Oxford Cryosystems has established a method of mapping the true temperature at 5 mm from the end of the nozzle. Data collection and processing were carried out using a *WinXPOW* package (Stoe & Cie, 2007).

The programs *WinGX* (Farrugia, 1999), *Mercury* (Macrae *et al.*, 2006), *PLATON* (Spek, 2009), *PowderCell* (Kraus & Nolze, 1999) were used for visualization and analysis. Hirshfeld surfaces were calculated using *CrystalExplorer* (Wolff *et al.*, 2007).

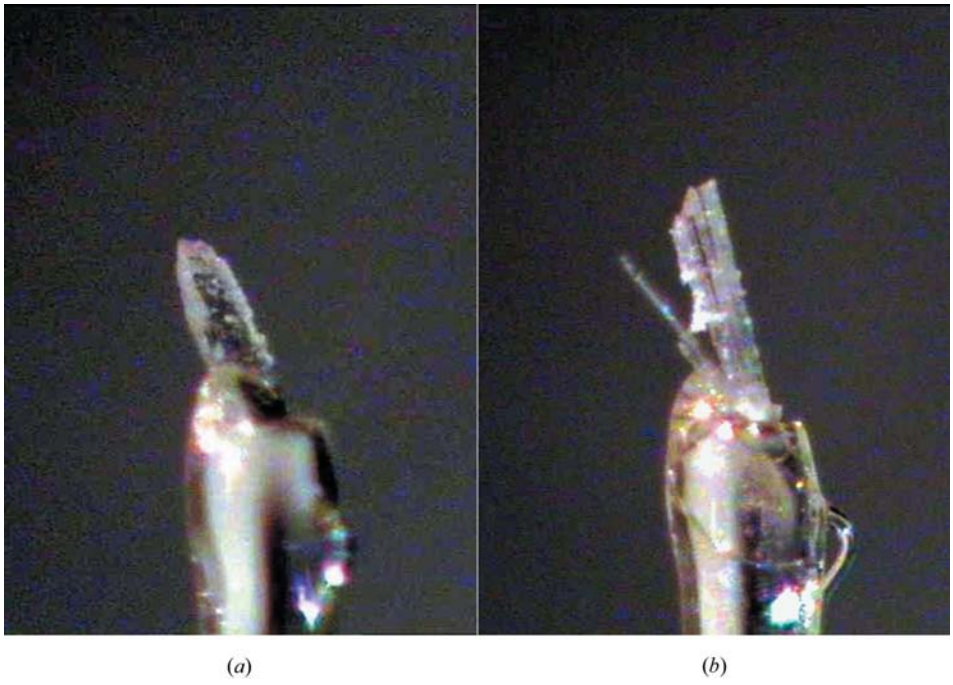

Figure 3
A photograph of the crystal of chlorpropamide (originally the ε-form) at 100 K, after the phase transition into the ε'-form has occurred for the first time (*a*), and at 200 K, after several cooling–heating cycles bringing the crystal through the phase transition point (*b*).

2.3. FT-IR spectroscopy

Variable-temperature (293–83 K, measurement precision 0.1 K) FT-IR spectra of the α- and ε-polymorphs of chlorpropamide pressed into thin platelets were measured using a FT-IR spectrometer (Digilab Excalibur 3100) with a transmission IR microscope UMA-400 (Varian) in the spectral range 4000–600 cm^{-1} at 4 cm^{-1} resolution. A variable-temperature FT-IR 600 Linkam stage with temperature controller was used. Cooling–heating was carried out in a 'ramp-hold' manner, with 10 or 20 K steps with the temperature changed at a rate of 10 K min^{-1} between the steps (the time of measuring one spectrum equal to 1–2 min).

3. Results and discussion

3.1. The $\varepsilon \leftrightarrow \varepsilon'$ phase transition in a single crystal: general notes

When the starting crystal of the ε-polymorph was cooled from ambient temperature down to 100 K, it transformed into a new polymorph, the single-crystal remaining intact and transparent (Fig. 3*a*). The phase transition went throughout the bulk of the crystal. The cell parameters of the new polymorph (termed the ε'-form) were similar to those of the previously known commercial α-form, but the space-group symmetry was the same as for the ε-form ($Pna2_1$), and differed from that for the α-form ($P2_12_12_1$; Table 2). On heating the ε'-form, a reverse transition occurred between 200 and 250 K (Fig. 2). The crystal structure of the ε-form was refined at 250 K. In the second cooling cycle the phase transition into the ε'-form was observed at 200 K (Fig. 2), and the crystal structure of this polymorph was refined at this temperature point. After the second cooling, the crystal split (Fig. 3*b*) and therefore the data quality at 200 K was worse than at 100 K. The orientation matrix fitted only approximately 50% of reflections. The remaining reflections corresponded to the crystallites with the same lattice cell, but different orientations (mainly a rotational disorder around the *b* axis was observed, but the crystallites rotated around other crystallographic axes were also observed). Multiple cooling–reverse heating cycling resulted in the complete fragmentation of the single crystal.

3.2. Crystal structure of the ε'-polymorph

As a result of the phase transition from the ε- to the ε'-form, the molecular conformation changed from type II to type I, *i.e.* the alkyl tail rotated by 171° (see the torsion angle values of C9—C8—N2—C7 in Table 3), preserving its *trans* conformation (see the torsion angle values of N2—C8—C9—C10 in Table 3 and Fig. 4). The conformation of the molecule in the ε'-polymorph became very close to that in the α-polymorph (Fig. 4), the difference in the values of the torsion angles not exceeding 3° (Table 3). In a previous publication (Drebushchak, Chukanov & Boldyreva, 2008), the orientation of the alkyl chain in the chlorpropamide molecule was correlated with the packing density, and the study of the $\varepsilon \rightarrow \varepsilon'$ transformation has confirmed that orientation (I) favors a denser packing than orientation (II) (Table 1).

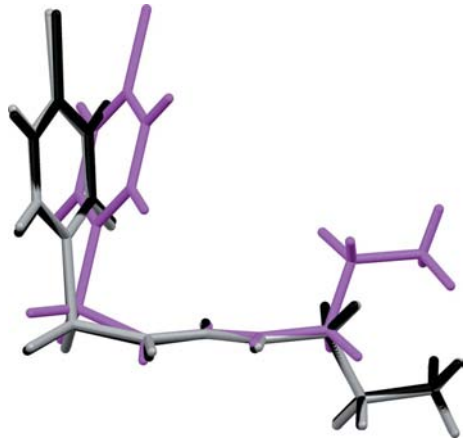

Figure 4
Overlay of the molecular structures of the three chlorpropamide polymorphs. Color scheme: magenta – ε-form, black – ε'-form, grey – α-form.

Table 4
Parameters (Å, °) for hydrogen bonds and short intermolecular contacts at several temperatures.

	D—H···A	D—H	H···A	D···A	D—H···A
ε-form,† 295 K					
(1)	N1—H1N···O3^{i}	0.86	2.02	2.726 (3)	138
(2)	N2—H2N···O2^{i}	0.86	2.36	3.026 (3)	134
(3)	N2—H2N···O3^{i}	0.86	2.31	3.054 (3)	144
	C2—H2···O1^{ii}	0.93	2.56	3.283 (4)	135
ε-form, 250 K					
(1)	N1—H1N···O3^{i}	0.87	2.02	2.718 (6)	136
(2)	N2—H2N···O2^{i}	0.87	2.35	3.013 (6)	134
(3)	N2—H2N···O3^{i}	0.87	2.30	3.044 (6)	144
	C2—H2···O1^{ii}	0.94	2.52	3.256 (8)	135
ε'-form, 200 K					
(1)	N1—H1N···O3^{iii}	0.88	1.92	2.774 (9)	162
(2)	N2—H2N···O2^{iii}	0.88	2.24	2.928 (10)	135
(3)	N2—H2N···O3^{iii}	0.88	2.27	3.038 (9)	146
	C10—H10*A*···O1^{iv}	0.98	2.58	3.404 (11)	142
	C2—H2···Cl1^{v}	0.95	2.84	3.643 (10)	143
ε'-form, 100 K					
(1)	N1—H1N···O3^{iii}	0.88	1.91	2.753 (5)	161
(2)	N2—H2N···O2^{iii}	0.88	2.23	2.910 (5)	134
(3)	N2—H2N···O3^{iii}	0.88	2.22	2.998 (5)	147
	C10—H10*A*···O1^{iv}	0.98	2.55	3.378 (5)	142
	C2—H2···Cl1^{v}	0.95	2.80	3.613 (5)	144
α-form, 295 K					
(1)	N1—H1N···O3^{vi}	0.86	1.95	2.781 (5)	164
(2)	N2—H2N···O2^{vi}	0.86	2.27	2.950 (5)	137
(3)	N2—H2N···O3^{vi}	0.86	2.31	3.067 (5)	147
	C10—H10*A*···O1^{vii}	0.96	2.51	3.332 (6)	143
α-form, 200 K					
(1)	N1—H1N···O3^{vi}	0.88	1.92	2.767 (4)	162
(2)	N2—H2N···O2^{vi}	0.88	2.23	2.923 (4)	135
(3)	N2—H2N···O3^{vi}	0.88	2.25	3.025 (4)	146
	C10—H10*A*···O1^{vii}	0.98	2.49	3.305 (5)	140
α-form, 105 K					
(1)	N1—H1N···O3^{vi}	0.88	1.91	2.757 (5)	161
(2)	N2—H2N···O2^{vi}	0.88	2.23	2.915 (5)	134
(3)	N2—H2N···O3^{vi}	0.88	2.23	3.003 (5)	146
	C10—H10*A*···O1^{vii}	0.98	2.46	3.282 (6)	141

Symmetry codes: (i) $-x+1, -y, z-\frac{1}{2}$; (ii) $x, 1+y, z$; (iii) $-x+1, -y+2, z-\frac{1}{2}$; (iv) $-x+1, -y+2, z+\frac{1}{2}$; (v) $-x+\frac{1}{2}, y-\frac{1}{2}, z-\frac{1}{2}$; (vi) $-x+\frac{1}{2}, -y+1, z+\frac{1}{2}$; (vii) $-x+\frac{1}{2}, -y+1, z-\frac{1}{2}$. † These values are given as a comparison from Drebushchak, Chukanov & Boldyreva (2008).

The change in the molecular conformation on the $\varepsilon \rightarrow \varepsilon'$ transformation (rotation of the aromatic ring and of the alkyl chain) was accompanied by the elongation of the shortest N—H···O hydrogen bond (1) (Fig. 1, Table 4). The bifurcated hydrogen bond [(2) and (3)] shortened as a result of the $\varepsilon \rightarrow \varepsilon'$ transformation. A short C10—H10*A*···O1^{iv} [symmetry code: (iv) $-x+1, -y+2, z+\frac{1}{2}$] contact between the methyl group of an alkyl tail and an O atom of the SO_2 group of a neighboring molecule in the same hydrogen-bonded ribbon (Table

Table 5
The coefficients of thermal expansion κ_l for the ε-, ε'- and α-polymorphs of chlorpropamide.

Polymorph	Along a κ_a (K^{-1}) $\times 10^{-4}$	Along b κ_b (K^{-1}) $\times 10^{-4}$	Along c κ_c (K^{-1}) $\times 10^{-4}$	κ_V (K^{-1}) $\times 10^{-4}$	Temperature interval (K)
ε-form	1.03 (2)	−0.05 (2)	−0.13 (2)	0.86 (4)	210–295
ε'-form	0.38 (2)	1.33 (2)	0.61 (2)	2.32 (5)	100–200
α-form	0.03 (2)	1.38 (3)	0.54 (2)	1.96 (4)	105–295

4) is observed in the ε'-form. A short C2—H2···O1^{ii} contact [symmetry code: (ii) $x, 1+y, z$] between the aromatic ring and the SO_2 group of a neighboring molecule in another hydrogen-bonded ribbon, in the stack along the crystallographic b axis (Table 4), is only present in the initial ε-form and disappears in the ε'-form; the same is true for the short contacts between the methyl group of an alkyl tail and the C=O group of the neighboring molecules in the same stack [C10···C7^{ii} = 3.79 (1) Å, C10···O1^{ii} = 3.97 (1) Å at 250 K; symmetry code: (ii) $x, 1+y, z$].

The z-shaped motif was preserved after the $\varepsilon \rightarrow \varepsilon'$ transition, but the distance between the ribbons in the stack (characterized by the cell parameter b) decreased sharply [at $\sim$ 30.03 (1)% on transition from the ε-form at 295 K to the ε'-form at 100 K], since the rotation of the alkyl chains, of the aromatic rings, and the changes in the C—H···O contacts (see above) allowed the molecules to approach each other more closely (Fig. 5). At the same time, the structure expanded at $\sim$ 32.76 (2)% along the crystallographic a direction, owing to the elongation of the molecules in this direction resulting from the rotation of the alkyl tails and aromatic rings. The c parameter (the direction of the hydrogen-bonded ribbons) remained practically constant [slightly decreased at 0.59 (1)%]. The total volume decrease during the transition from the ε-form at 295 K to the ε'-form at 100 K was equal to 7.66 (2)% (Fig. 2). The Hirshfeld surfaces fingerprint plots (McKinnon *et al.*, 2004, 2007) have revealed a pronounced difference between the intermolecular contacts in the ε- and the ε'-polymorphs, firstly in the H···Cl contacts (Figs. 6*a* and *b*). The short contacts C2—H2···Cl1^{v} [Table 4, symmetry code: (v) $-x+\frac{1}{2}, y-\frac{1}{2}, z-\frac{1}{2}$] between the molecules from different hydrogen-bonded ribbons are present only in the ε'-polymorph.

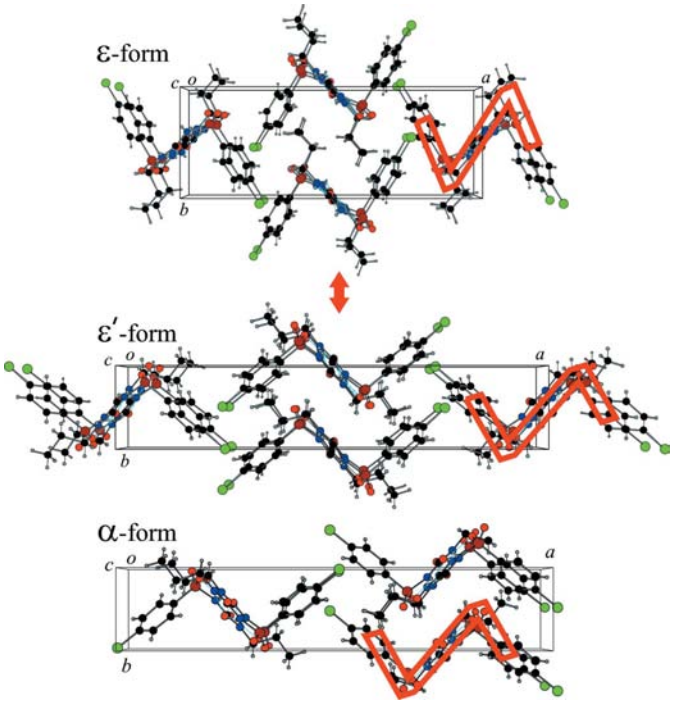

Figure 5
Fragments of the crystal structures of the ε-form, the ε'-form, and, for comparison, the stable α-form. A hydrogen-bonded ribbon with the z-shaped motif is outlined in red.

3.3. Comparison of the structures of ε'- and α-polymorphs

The new ε'-polymorph is similar to the commercial α-form in the molecular conformations, the z-shaped motif and the cell parameters (Figs. 2, 4 and 5, and Tables 1–4). Still, the two forms are different in space-group symmetry, and this difference is reliably revealed by single-crystal X-ray diffraction.[2] The Hirshfeld surface fingerprint plots (McKinnon *et al.*, 2004, 2007) have also shown a pronounced difference in the intermolecular contacts in the ε'- and α- polymorphs (Figs. 6*b* and *c*). In particular, in the α-polymorph the short C—H···Cl contacts are absent.

The packing of the z-shaped ribbons in the ε'-form is the same as in the ε-polymorph from which it is formed as a result of a solid-state transformation on cooling, but differs from that in the thermodynamically stable α-polymorph: in the ε- and ε'-forms the neighboring ribbons are related by the glide planes, whereas in the α-form they are related by screw axes 2_1 (Fig. 7). A transformation of the ε'-polymorph into the α-form would require the molecules to be inverted into their mirror images in every second ribbon. At low temperature this transformation is kinetically hindered and therefore on cooling the ε-form transforms into the ε'-form, and on reverse heating the crystal structure of the ε'-polymorph prefers to go back to the metastable ε-form rather than to the thermodynamically stable α-polymorph. The rotation of the alkyl tail by 171° in the crystal structure of ε- and ε'-polymorphs must have a lower barrier than that of the inversion of a molecule into its mirror image. This agrees with the recent NMR studies of the relative barriers for the motions of various molecular fragments in the chlorpropamide molecule – lowest for the motions of the alkyl tails and highest for the motion of the propylaminocarbonyl group (S—N axis; Wasicki *et al.*, 2009).

[2] An attempt to solve the crystal structure after the low-temperature phase transition in the space group of the α-form $P2_12_12_1$ fails, a refinement of the structure starting from the model of the α-polymorph diverges.

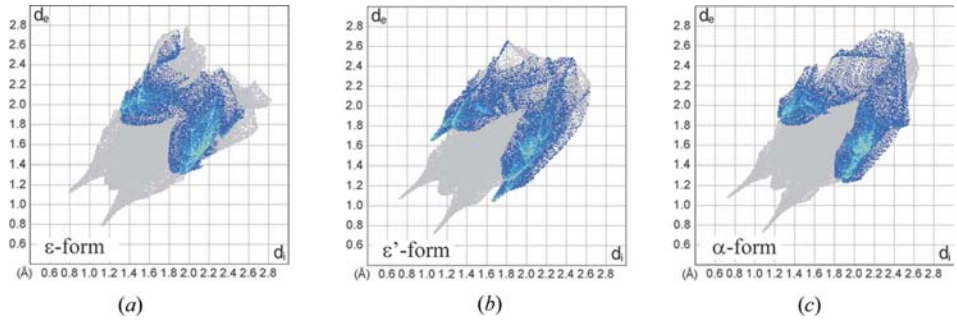

Figure 6
Hirshfeld surfaces fingerprint plots for (*a*) the ε-form, (*b*) the ε′-form, and, for comparison, (*c*) the stable α-form. The H···Cl contacts are shown in shades of blue; the full fingerprint appears as a gray shadow.

In the previous publications, the ε-polymorph was reported to transform slowly and irreversibly into the stable α-form on storage at ambient and higher temperatures (De Villiers & Wurster, 1999; Sonoda *et al.*, 2004; Chesalov *et al.*, 2008). The reversible $\varepsilon \leftrightarrow \varepsilon'$ transformation is assumed to be either an alternative path under 'mild transformation conditions', or a 'transient state' of the irreversible $\varepsilon \rightarrow \alpha$ transition resulting in a more radical structural reconstruction.

3.4. Anisotropy of the lattice strain in the ε-, ε′- and α-polymorphs on cooling

Analysis of the anisotropy of lattice strain on cooling may be informative for understanding the intermolecular interactions in the crystal structure (Boldyreva *et al.*, 1997*a*,*b*, 2004; Drebushchak, Kolesnik & Boldyreva, 2006; Drebushchak, Boldyreva & Mikhailenko, 2008*a*,*b*). In the case of the ε-, ε′- and α-polymorphs, the three phases could not be studied in the same temperature range. Therefore, to compare the relative linear strain in the different polymorphs, we have averaged the strain values obtained in different temperature intervals for each polymorph having calculated the values of the thermal expansion coefficient κ_l as

$$\kappa_l = \frac{1}{l}\frac{\Delta l}{\Delta T}, \qquad (1)$$

where l are the values of a, b, c or V. It is conventional to use 'α' for the coefficient of thermal expansion, but here we use 'κ' to avoid the confusion with the polymorph identifier. The values of κ_l could then be compared for the polymorphs existing in different temperature ranges (Table 5).

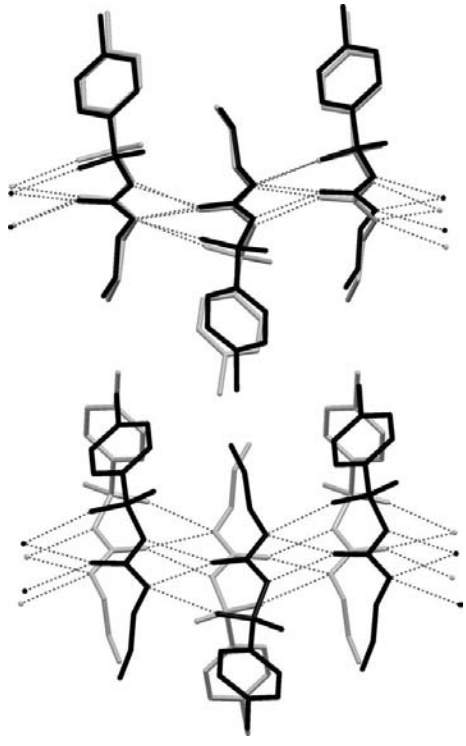

Figure 7
Structural overlay of the two neighboring ribbons of the ε′-form, and the stable α-form. Color scheme: black – ε′, grey – α.

It is especially interesting to compare the strain in the crystallographic direction b, normal to the z-type ribbons for different polymorphs (Fig. 5, Table 5). The ε-polymorph is almost incompressible in the b direction on cooling prior to the transition point, because the short contacts between the aromatic rings and the alkyl tails of the neighboring molecules in a stack do not allow the molecules to approach each other. The maximum compression of the ε-polymorph is along a. The bulk strain of the ε-form on cooling is smaller than those of the α- and ε′-forms, although the ε-form has the lowest density among all the polymorphs. During the phase transition into the ε′-form, the structure compresses discontinuously along the b axis and expands along the a axis, after which the major compression of the ε′-form is observed along the b axis since the alkyl tails have rotated. In other directions the structure is much more rigid. The anisotropy of lattice strain of the α-polymorph on cooling is similar to that of the ε′-form (Table 5). The structure of the α-polymorph is almost not compressed along the a direction on cooling. The chlorpropamide molecules are stretched in this direction [the difference in the x coordinates of Cl1 and C8 at 295 K is 8.460 (2) Å, and at 105 K – 8.487 (2) Å]. This elongation of molecules compensates for a decrease in the distance between the molecules. A similar effect has been previously observed for other structures, sometimes even resulting in the negative linear thermal expansion coefficients (Drebushchak & Boldyreva, 2004; Boldyreva *et al.*, 2004; Drebushchak, Kolesnik & Boldyreva, 2006; Drebushchak, Boldyreva & Mikhailenko, 2008*a*,*b*).

3.5. The ε ↔ ε′ polymorphic transition in the powder samples

Since the early 1970s, vibrational spectroscopy has been widely used to distinguish between the 'forms' of chlorprop-

amide, and even to estimate the relative contents of different forms in a mixture (see for example Simmons *et al.*, 1973; Tudor *et al.*, 1993; Mehrens *et al.*, 2005). Our recent theoretical and experimental analysis of the IR and Raman spectra of the five polymorphs of chlorpropamide (Chesalov *et al.*, 2008) has shown these vibrational spectra to be sensitive to the molecular conformations, hydrogen-bond lengths, and the z- or π-type hydrogen-bonded ribbons. Therefore, we decided to follow the $\varepsilon \leftrightarrow \varepsilon'$ polymorphic transition by IR spectroscopy. For this study we had to use a powder sample.

On cooling the sample from 303 K down to 123 K, the IR spectra changed continuously (Figs. 8*a* and *b*, spectra 1 and 2): the half-widths of the bands decreased and the shifts of their maxima did not exceed 10 cm^{-1}. The largest shifts were observed for the vibrations of the functional groups directly involved in the formation of hydrogen bonds, especially of the NH groups. The decrease in frequencies of the NH-stretching vibrations (Fig. 9), and the increase in frequencies of the bending vibrations of the two imine groups indicate the strengthening of the hydrogen bonds. Changes in the frequencies of vibrations of molecular fragments not participating in hydrogen bonds did not exceed 2–3 cm^{-1}.

The first indications of the $\varepsilon \rightarrow \varepsilon'$ transition on cooling appeared in the FT-IR spectra at 113 K. In the measured spectral range discontinuous changes in the number of vibrational bands, their relative intensities and positions of the maxima were observed (Fig. 8, spectrum 3; Fig. 9), which are related to the changes in the molecular conformations and the intermolecular hydrogen bonding. The most pronounced differences could be observed in the spectral range of the overtones or combination frequencies (2000–1700 cm^{-1}; Figs. 8*c* and *d*), and this spectral range is the best one to distinguish between the different chlorpropamide polymorphs based on

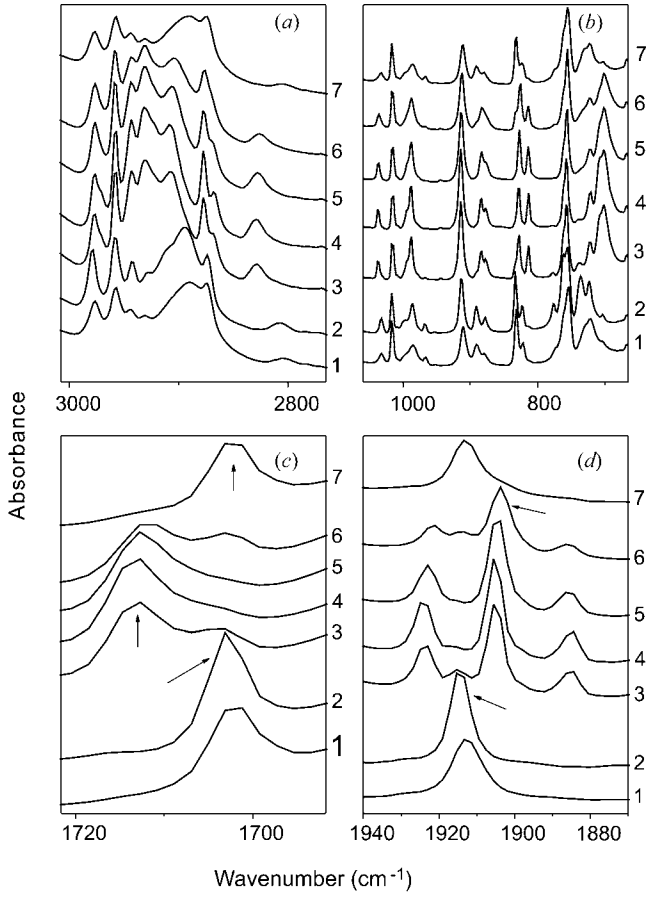

Figure 8
Changes in the IR spectra of the ε-form of chlorpropamide in selected spectral regions on cooling (1–303, 2–173, 3–113 and 4–83 K) and subsequent heating (5–173, 6–243 and 7–283 K). Arrows show the most pronounced changes.

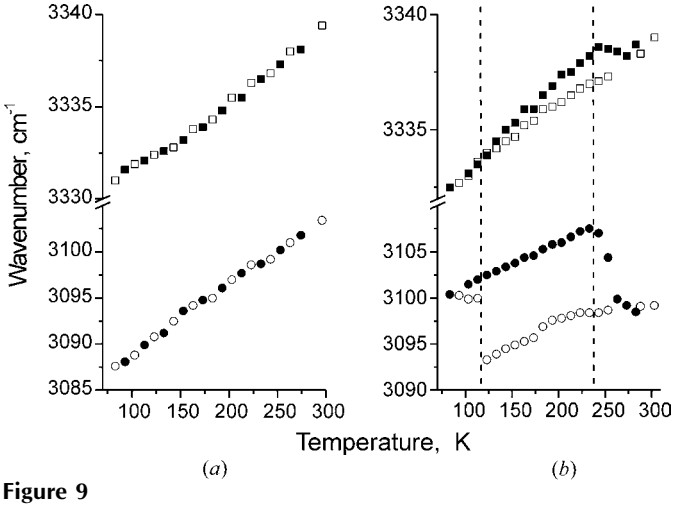

Figure 9
Temperature dependence of the position of the NH stretching modes of (*a*) the α-polymorph and (*b*) $\varepsilon(\varepsilon')$-polymorphs of chlorpropamide. Open symbols – cooling, black symbols – heating, squares – high-frequency ν(NH) band, circles – low-frequency ν(NH) band.

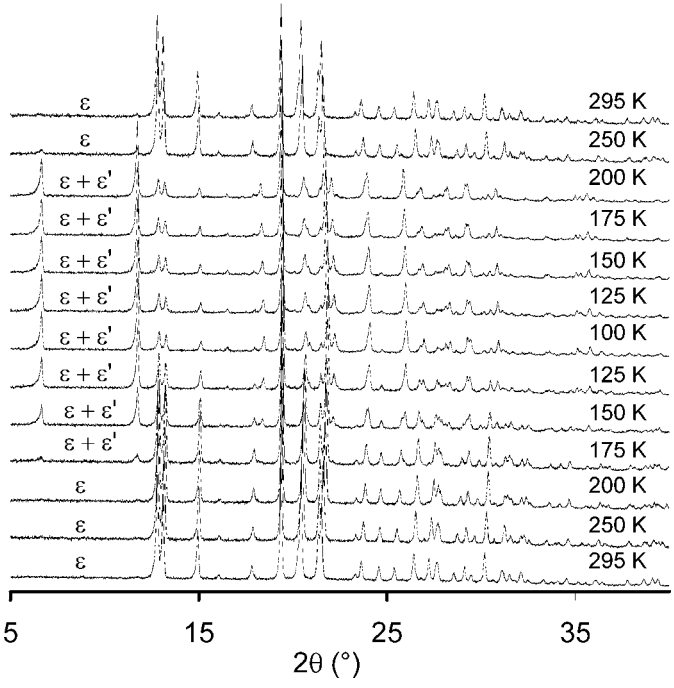

Figure 10
Powder diffraction patterns of the original ε-form measured at different temperatures through the $\varepsilon \leftrightarrow \varepsilon'$ phase transition (from the bottom upwards).

vibrational spectra (Chesalov *et al.*, 2008). The weak vibrational bands of the ε-form could be still observed down to 83 K (the lowest temperature achieved), the reverse transition on heating started at 223 K, but the weak bands of the ε'-form could be observed until 263 K (Fig. 8).

The IR study of the polycrystalline sample has revealed the inhomogeneity of the $\varepsilon \leftrightarrow \varepsilon'$ transition throughout the sample, resulting in the co-existence of the two polymorphs in a wide temperature range. This inhomogeneity manifested itself in the spectra as an increase in the scattering background at the transition point due to the inhomogeneous distribution of the refractive index throughout the sample bulk, and possibly also due to the existing distribution in the particle size. The same effect (the co-existence of the two polymorphs in a wide temperature range) could be observed in the study of a powder sample by variable-temperature X-ray diffraction (Fig. 10). The peaks related to the appearance of the new ε'-form could be observed on cooling down to 175 K, and practically disappeared on reverse heating up to 250 K. The transformation was not complete throughout the powder sample: the peaks of the starting ε-polymorph could be observed at least down to 100 K (the lowest temperature achieved).[3]

The study of the $\varepsilon \leftrightarrow \varepsilon'$ phase transition in a powder sample has also shown that the IR spectrum (Figs. 11*a* and *b*) and the X-ray powder diffraction patterns (Fig. 12) of the powders of the ε'- and the α-polymorphs are rather similar, although not identical. Vibrational spectroscopy may not allow the ε'- and the α-polymorphs to be distinguished unambiguously if they are present in a mixture with other forms, since the major differences between the spectra of these two forms are related to very weak bands in the 2000–1700 cm^{-1} range (Figs. 11*c* and *d*).

Based on the calculations using the structure models derived from the single-crystal data (Stoe & Cie, 2007), the main differences in the powder diffraction patterns of the α- and the ε'-forms can only be noticed in the higher 2θ angle range, while the positions and the relative intensities of the peaks below $2\theta = 19^\circ$ (Cu $K\alpha$ radiation) are almost identical (Fig. 12). The differences in the powder diffraction patterns related to different reflection conditions in the $Pna2_1$ and in the $P2_12_12_1$ space groups can hardly be noticed if only a small amount of the α- or the ε'-form is available (*e.g.* when present as an admixture to another polymorph in a powder sample), since the intensities of 'extra' peaks in the pattern of the α-form are low. The differences in the relative intensities of the peaks in powder diffraction patterns of the ε' and α-forms can be masked by preferred orientation effects. In this respect, it is worth noting that the commonly used experimental technique of estimating the content of the α-polymorph of chlorpropamide in a mixture with other polymorph(s) from the integral intensity of 1–2 low-angle diffraction peaks in the powder diffraction pattern (at 2θ about 12° for Cu $K\alpha$) (Otsuka *et al.*, 1989; Cao *et al.*, 2002; Wildfong *et al.*, 2005; Koivisto *et al.*,

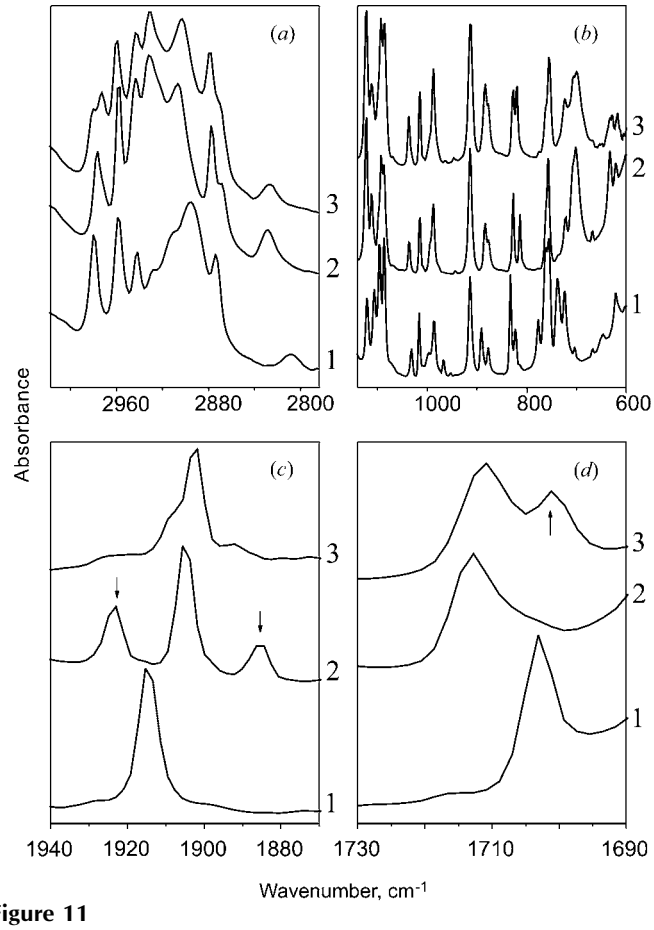

Figure 11
IR spectra of the ε- (1), ε'- (2) and α-forms (3) of chlorpropamide in the selected spectral ranges. Arrows show the main differences.

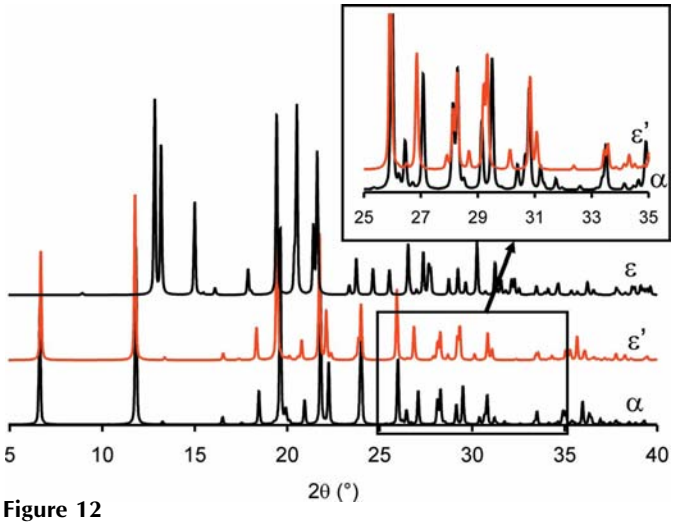

Figure 12
Powder diffraction patterns of the ε-, ε'- and α-polymorphs of chlorpropamide calculated from the models based on single-crystal diffraction data. The large-angle range is magnified to show the differences between the ε'- and the α-forms.

[3] As can be seen, the temperatures, at which the start and the end of the $\varepsilon \leftrightarrow \varepsilon'$ transition were registered by different techniques, are somewhat different, but a straightforward comparison of these values is hardly possible since it may not only be related to the difference in the samples, but maybe also due to some difference in the actual temperature values at the sample itself in the different experimental set-ups (heating was stepwise).

2006) may lead to the wrong conclusions, since the same peaks are also present in the powder diffraction pattern of the ε'-polymorph, and the two forms may be easily confused. Even a full-profile analysis taking into account the preferred orientation effects may lead to disputable conclusions, if the amount of the α- (or ε'-) form in the mixture is small.

4. Conclusions

The $\varepsilon \leftrightarrow \varepsilon'$ polymorphic transition in chlorpropamide on cooling is an interesting example of a reversible conformational transformation, during which the molecular packing, the hydrogen-bond pattern and the space-group symmetry are preserved. The structure becomes denser as a result of the transition and, at the same time, the originally short intermolecular hydrogen bonds become longer. As a result of the transformation one metastable polymorph (ε) transforms reversibly into another metastable polymorph (ε'), whereas the irreversible transition into the thermodynamically stable form (α) is kinetically hindered since it would require every second ribbon of the hydrogen-bonded molecules in the crystal structure to be inverted. Since the cell parameters in the stable (α) and newly discovered metastable (ε') polymorphs are similar, and the main difference between the two structures is in the packing of the rather similar z-shaped ribbons, resulting in a different space-group symmetry, it is not trivial to distinguish between the two polymorphs, using IR spectroscopy or X-ray powder diffraction, especially if they are present in a mixture with other forms. At the same time, the differences between the spectra and the powder patterns of the pure α- and ε'-forms are sufficient to identify the polymorph reliably after careful analysis. The single-crystal to single-crystal phase transition is sharp and proceeds throughout the bulk of the sample. At the same time, in the polycrystalline samples the same phase transition starts and ends at different temperatures in different particles, and as a result the two phases co-exist in a wide temperature range.

This work was supported by grants from BRHE (RUX0-008-NO-06), by Integration Project No. 110 of the Siberian Branch of RAS, the Innovation Project of Rosobrazovanie No. 456, and grant No. 08-03-00143 from RFBR.

References

Al-Saieq, S. S. & Riley, G. S. (1982). *Pharm. Acta Helv.* **57**, 8–11.

Bernstein, J. (2002). *Polymorphism in Molecular Crystals.* IUCr Monographs on Crystallography. Oxford University Press.

Boldyreva, E. V., Drebushchak, T. N., Shakhtshneider, T. P., Sowa, H., Ahsbahs, H., Goryainov, S. V., Ivashevskaya, S. N., Kolesnik, E. N., Drebushchak, V. A. & Burgina, E. B. (2004). *Arkivoc*, **XII**, 128–155.

Boldyreva, E., Kivikoski, J. & Howard, J. A. K. (1997*a*). *Acta Cryst.* B**53**, 394–404.

Boldyreva, E., Kivikoski, J. & Howard, J. A. K. (1997*b*). *Acta Cryst.* B**53**, 405–414.

Brittain, H. G. (1999). Editor. *Polymorphism in Pharmaceutical Solids.* New York: Marcel Dekker.

Burger, A. (1975). *Sci. Pharm.* **43**, 152–161.

Cao, W., Bates, S., Peck, G. E., Wildfong, P. L. D., Qiu, Z. & Morris, K. R. (2002). *J. Pharm. Biomed. Anal.* **30**, 1111–1119.

Chesalov, Yu. A., Baltakhinov, V. P., Drebushchak, T. N., Boldyreva, E. V., Chukanov, N. V. & Drebushchak, V. A. (2008). *J. Mol. Struct.* **891**, 75–86.

De Villiers, M. M. & Wurster, D. E. (1999). *Acta Pharm.* **49**, 79–88.

Drebushchak, T. N. & Boldyreva, E. V. (2004). *Z. Kristallogr.* **219**, 506–512.

Drebushchak, T. N., Boldyreva, E. V. & Mikhailenko, M. A. (2008*a*). *J. Struct. Chem.* **49**, 84–94.

Drebushchak, T. N., Boldyreva, E. V. & Mikhailenko, M. A. (2008*b*). *Z. Strukt. Khim.* **49**, 90–100.

Drebushchak, T. N., Chukanov, N. V. & Boldyreva, E. V. (2006). *Acta Cryst.* E**62**, o4393–o4395.

Drebushchak, T. N., Chukanov, N. V. & Boldyreva, E. V. (2007). *Acta Cryst.* C**63**, o355–o357.

Drebushchak, T. N., Chukanov, N. V. & Boldyreva, E. V. (2008). *Acta Cryst.* C**64**, o623–o625.

Drebushchak, V. A., Drebushchak, T. N., Chukanov, N. V. & Boldyreva, E. V. (2008). *J. Therm. Anal. Calorim.* **93**, 343–351.

Drebushchak, T. N., Kolesnik, E. N. & Boldyreva, E. V. (2006). *Z. Kristallogr.* **221**, 128–138.

Farrugia, L. J. (1999). *J. Appl. Cryst.* **32**, 837–838.

Flack, H. D. (1983). *Acta Cryst.* A**39**, 876–881.

Hilfiker, R. (2006). *Polymorphism in the Pharmaceutical Industry.* Weinheim: Wiley-VCH.

Koo, C. H., Cho, S. I. & Yeon, Y. H. (1980). *Arch. Pharmacol. Res.* **3**, 37–49.

Koivisto, M., Heinänen, P., Tanninen, V. P. & Lehto, V.-P. (2006). *Pharm. Res.* **23**, 813–820.

Kraus, W. & Nolze, G. (1999). *Powder Cell Software*, Version 2.4. Federal Institute for Material Research and Testing, Berlin, Germany.

Macrae, C. F., Edgington, P. R., McCabe, P., Pidcock, E., Shields, G. P., Taylor, R., Towler, M. & van de Streek, J. (2006). *J. Appl. Cryst.* **39**, 453–457.

McKinnon, J. J., Jayatilaka, D. & Spackman, M. A. (2007). *Chem. Commun.* **37**, 3814–3816.

McKinnon, J. J., Spackman, M. A. & Mitchell, A. S. (2004). *Acta Cryst.* B**60**, 627–668.

Mehrens, S. M., Kale, U. J. & Qu, X. (2005). *J. Pharm. Sci.* **94**, 1354–1367.

Otsuka, M., Matsumoto, T. & Kaneniwa, N. (1989). *J. Pharm. Pharmacol.* **41**, 665–669.

Oxford Diffraction (2008*a*). *CrysAlis CCD.* Oxford Diffraction Ltd, Abingdon, England.

Oxford Diffraction (2008*b*). *CrysAlis RED.* Oxford Diffraction Ltd, Abingdon, England.

Sheldrick, G. M. (2008). *Acta Cryst.* A**64**, 112–122.

Simmons, D. L., Ranz, R. J. & Gyanchandani, D. (1973). *Can. J. Pharm. Sci.* **8**, 125–127.

Sonoda, Y., Hirayama, F., Arima, H. & Uekama, K. (2004). *J. Inclusion Phenom.* **50**, 73–77.

Spek, A. L. (2009). *Acta Cryst.* D**65**, 148–155.

Stoe & Cie (1997*a*). *Stadi*4. Stoe & Cie GmbH, Darmstadt, Germany.

Stoe & Cie (1997*b*). *X-RED.* Stoe & Cie GmbH, Darmstadt, Germany.

Stoe & Cie (2007). *WinXPOW*. Stoe & Cie GmbH, Darmstadt, Germany.

Tudor, A. M., Church, S. J., Hendra, P. J., Davies, M. C. & Melia, C. D. (1993). *Pharm. Res.* **10**, 1772–1776.

Ueda, H., Nambu, N. & Nagai, T. (1984). *Chem. Pharm. Bull.* **32**, 244–250.

Vemavarapu, C., Mollan, M. J. & Needham, T. E. (2002). *Am. Assoc. Pharm. Sci. PharmSciTech* **3**, 29, http://www.aapspharmscitech.org.
Wasicki, J., Kozlenko, D. P., Pankov, S. E., Bilski, P., Pajzderska, A., Hancock, B. C., Medek, A., Nawrocik, W. & Savenko, B. N. (2009). *J. Pharm. Sci.* **98**, 1426–1437.
Wildfong, P. L. D., Morley, N. A., Moore, M. D. & Morris, K. R. (2005). *J. Pharm. Biomed. Anal.* **39**, 1–7.
Wolff, S. K., Grimwood, D. J., McKinnon, J. J., Jayatilaka, D. & Spackman, M. A. (2007). *CrystalExplorer*2.1. University of Western Australia, http://hirshfeldsurface.net/CrystalExplorer.